



Cite this: *RSC Adv.*, 2020, 10, 17951

Received 27th December 2019

Accepted 30th April 2020

DOI: 10.1039/c9ra10962e

rsc.li/rsc-advances

Synergetic catalysis of a cobalt-based coordination polymer for selective visible-light driven CO₂-to-CO conversion†

Sheng-Jie Li, Yong-Bin Chang, Ming Li, You-Xiang Feng and Wen Zhang *

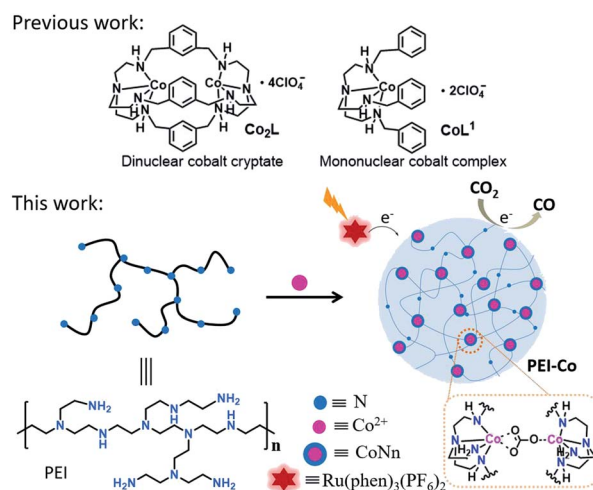
Herein, based on the strategy of synergetic catalysis, we report a cobalt-based coordination polymer PEI₆-Co. As a heterogeneous catalyst, PEI₆-Co shows a selectivity of 95% and a yield of 1170 mmol g⁻¹ for visible-light-driven CO₂-to-CO conversion in a water containing system, which is almost 2.8 times that of the mononuclear cobalt catalyst CoL¹ and is comparable to that of the dinuclear cobalt catalyst Co₂L.

Energy shortages and greenhouse gas emissions caused by the consumption of fossil fuels have become an indisputable obstacle to the sustainable development of human beings. Solar-driven conversion of CO₂ to carbon fuels is regarded as an ideal strategy to deal with these energy and environmental issues.^{1–7} In this context, many researchers have devoted themselves to promote the activity and efficiency of photocatalytic CO₂ conversion.^{8–11} Unlike the reduction of H₂O to H₂, the CO₂ reduction reactions are more complicated. Firstly, CO₂ is an inert molecule, it requires high energy to be activated. Secondly, as the carbon atom in CO₂ is the highest valence, various reduction products including CO,¹² formic acid,¹³ formaldehyde,¹⁴ methane¹⁵ and some multi-carbon products¹⁶ can be obtained. Besides, due to the competitive reduction of protons, the selectivity of CO₂ reduction is usually low in water containing medium.¹⁷ In this context, the development of a catalyst for the efficient and highly selective reduction of CO₂ to a single valuable product is still challenging, especially in water containing system.

In recent decades, many molecular catalysts for the reduction of CO₂ have been designed elaborately. For example, the catalysts based on Ru,^{18,19} Re,^{20,21} Ir,²² Fe,^{23,24} Co,^{25,26} Ni,^{27,28} Mn,²⁹ etc., have been developed to reduce CO₂ and the mechanisms for the activation and conversion of CO₂ have also been investigated reasonably.^{30,31} Notable among them is dinuclear metal synergistic catalysis (DMSC) in which two active centers are involved into the catalytic reaction concurrently and used to decrease the reaction barriers.^{32–34} In our previous works,²⁵ dinuclear cobalt cryptate Co₂L (Scheme 1) which was composed of aza-cryptand ligand and two adjacent cobalt ions displayed

excellent performance in the conversion of CO₂ to CO. Due to the immobilization and synergistic catalysis of two adjacent cobalt active sites to CO₂ molecules, the selectivity and the turnover numbers (TON) of Co₂L reached as high as 98%, and 16 896, respectively. Although molecular catalysts are significant in the study of catalytic mechanism and optimizing catalyst structure, the synthesis operations of such molecular catalyst are tedious and not conducive to its large-scale practical applications.

Herein, we choose polyethyleneimine (PEI) as the analogue of aza-cryptand and synthesize a cobalt-based coordination polymer (PEI₆-Co) as a heterogeneous catalyst for the photocatalytic reduction of CO₂ (Scheme 1). The reason for choosing PEI as a ligand is that both the structures of aza-cryptand and PEI have secondary amine and tertiary amine groups which can coordinate with Co²⁺. The formation of the coordination polymer can shorten the distance between cobalt active sites, which



Scheme 1 The structures of Co₂L, CoL¹, PEI-Co and the proposed catalysis process of PEI-Co for CO₂-to-CO conversion.

MOE International Joint Laboratory of Materials Microstructure, Institute for New Energy Materials and Low Carbon Technologies, School of Material Science and Engineering, Tianjin University of Technology, Tianjin 300384, China. E-mail: zhangwen@email.tjut.edu.cn

† Electronic supplementary information (ESI) available: Including XPS, CV, HRMS (ESI), UV absorption spectrum. See DOI: 10.1039/c9ra10962e



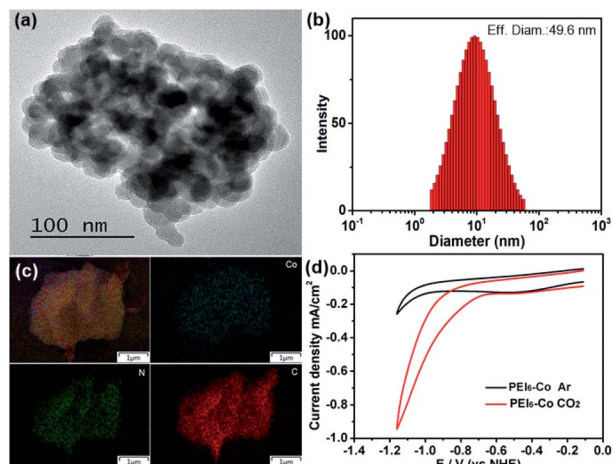


Fig. 1 (a) TEM image of PEI₆-Co. (b) DLS data of PEI₆-Co. (c) Mapping images of PEI₆-Co. (d) CV curves of PEI₆-Co in CH₃CN/H₂O (4 : 1) solution under an Ar (black) and CO₂ atmosphere (red) at 25 °C.

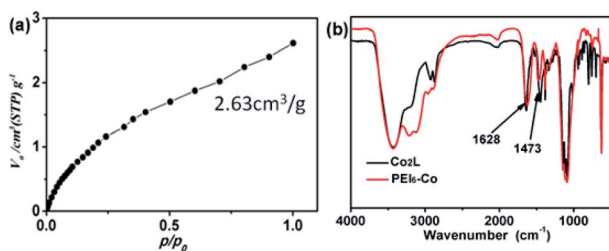


Fig. 2 (a) The adsorption curve for carbon dioxide of PEI₆-Co. (b) IR spectra of PEI₆-CO (red) and Co₂L (black) after adsorption of CO₂.

Table 1 Comparison of photocatalytic carbon dioxide reduction of PEI_x-Co^a

Entry	Catalyst	n_{H_2} (μmol)	n_{CO} (μmol)	Selectivity of CO	Activity (mmol g ⁻¹)
1	PEI ₄ -Co	0.35	4.35	93%	870
2	PEI ₅ -Co	0.36	4.71	93%	942
3	PEI ₆ -Co	0.34	5.84	95%	1170
4	PEI ₇ -Co	0.30	5.09	96%	1020
5	PEI ₈ -Co	0.26	4.90	95%	981

^a Reaction conditions: PEI_x-Co (5 μg), [Ru(phen)₃](PF₆)₂ (0.4 mM), TEOA (0.3 M), 5 mL CH₃CN/H₂O (v/v = 4 : 1) solution, 25 °C, 12 h. 450 nm LED lamp (100 mW cm⁻², irradiation area 0.8 cm²).

is similar to that of Co₂L, so that they may function synergistically in the photocatalytic reactions. Besides, PEI has been commonly used as a CO₂ absorbent in the past research of electrocatalytic reduction of CO₂.³⁵ As a result, when PEI₆-Co is used as a heterogeneous catalyst for the reduction of CO₂ in water containing system, the selectivity for CO reaches up to 95%, and the yield for CO₂-to-CO conversion reaches 1170 mmol g⁻¹, which is almost 2.8 times of molecular catalyst mononuclear cobalt CoL¹ and comparable with that of dinuclear cobalt catalyst Co₂L.

Co₂L and CoL¹ were prepared according to the literature.²⁵ PEI_x-Co (x represents the N/Co ratio) was synthesized through the coordination between the amine groups of PEI and cobalt ions and the exact contents of cobalt in the catalyst are listed in Table S1 (see ESI†). At the beginning, the formation of PEI₆-Co was characterized by TEM, DLS, element mapping, XPS and cyclic voltammetry measurements. As shown in Fig. 1a, PEI₆-Co was formed as a nanoparticle which resulted from the coordination crosslinking between the amino groups of PEI and Co ions. DLS measurement in Fig. 1b shows that the average diameter of this nanocomposite is about 50 nm. The elemental mapping images confirm that the Co, N and C elements uniformly distributed over the nanostructures of PEI₆-Co (Fig. 1c). The XPS measurement shows that there are only Co, N, C, O and Cl element in PEI₆-Co (Fig. S1†). These results indicate that amine groups in the PEI chain can coordinates with the cobalt ions, causing the long chain of the PEI to be twisted and crosslinked to form nanoparticles and giving the chance for cobalt centers to get closer. Besides, the redox property of PEI₆-Co was investigated using cyclic voltammogram (CV). The results in Fig. 1d show that compared with the CV curve under argon condition, the current has an obvious enhancement under CO₂ atmosphere and the onset potential ($E_{\text{onset}} = -0.62$ V vs. NHE) is more negative than that of Co₂L ($E_{\text{onset}} = -0.68$ V vs. NHE, Fig. S2†) and CoL¹ ($E_{\text{onset}} = -0.76$ V vs. NHE, Fig. S3†), indicating that PEI₆-Co can reduce CO₂ more easily than Co₂L and CoL¹. Besides, the redox potential of photosensitizer [Ru(phen)₃]^{3+/2+}* was reported as -0.84 V vs. NHE,²⁶ which is more negative than the onset potential of PEI₆-Co to CO₂ reduction, thus, it is feasible for [Ru(phen)₃](PF₆)₂ to donate electrons to PEI₆-Co under light irradiation, which is one of the foundations for driving the reduction of CO₂.

In addition, to examine the gathering ability of PEI₆-Co to CO₂, CO₂ adsorption experiment was carried out. As shown in Fig. 2a, PEI₆-Co has an adsorption capacity of 2.63 cm³ g⁻¹ towards CO₂. The IR spectra in Fig. 2b shows that after the treatment of CO₂ atmosphere, both PEI₆-Co and Co₂L have two peaks at 1628 cm⁻¹ and 1473 cm⁻¹, which belong to the stretching vibrations of the carbonate group. All these results indicate that PEI₆-Co, just like the molecular catalyst binuclear cobalt Co₂L, has the ability of adsorbing CO₂, which is favorable for the reduction of CO₂ in the heterogeneous catalysis process.

Encouraged by the positive results above, we optimized the atom ratio of N and Co in the catalysts for the reduction of CO₂. In the photoreaction system, the reaction solutions were prepared by adding photocatalyst PEI_x-Co and photosensitizer [Ru(phen)₃](PF₆)₂ to CH₃CN/H₂O (v/v = 4 : 1) solutions with triethanolamine (TEOA) as a reducing agent. The quartz reaction bottle was sealed by the rubber tube and filled with CO₂ for 30 min, then, followed by the irradiation of a 450 nm LED light. With the increase of N/Co ratio in the catalyst, the yield of CO product shows a volcano-type trend (Table 1). The highest yield of 1170 mmol g⁻¹ for CO is achieved when the ratio between N and Co reaches 6 : 1. This result indicates that the appropriate coordination structure is feasible for the reduction of CO₂. When the ratio of N/Co is low (entries 1 and 2), the uncoordinated N atoms is insufficient to adsorb CO₂. While too



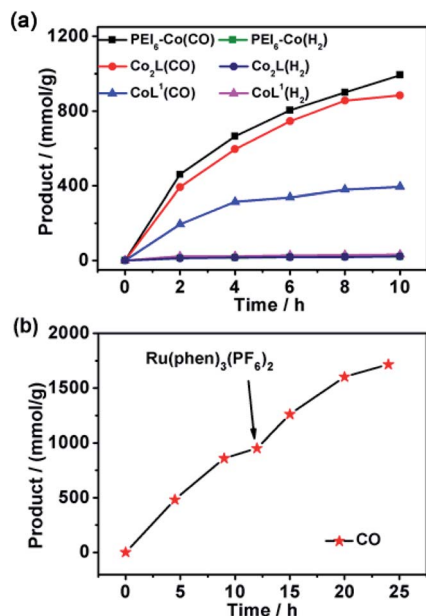


Fig. 3 (a) Comparison of photocatalytic carbon dioxide reduction yield of PEI₆-Co, Co₂L and CoL¹. (b) Stability test of PEI₆-Co.

Table 2 Photocatalytic carbon dioxide reduction control experiment of PEI₆-Co

Entry	n_{H_2} (μmol)	n_{CO} (μmol)	Selectivity of CO (%)	Activity (mmol g^{-1})
1 ^a	0	0.17	100%	34
2 ^b	0	0	—	0
3 ^c	0	0	—	0
4 ^d	0	0	—	0
5 ^e	0	0	—	0
6	0.34	5.84	95%	1170

^a No PEI₆-Co. ^b No TEOA. ^c No photosensitizer. ^d No light. ^e 100% Ar.

much N atoms would saturate the cobalt center and prevent it from acting as an active center to catalyze CO₂ reduction (entries 4 and 5). Besides, in the liquid phase, only trace amount of formate ($\sim 0.4 \mu\text{mol}$) was detected by ion chromatograph (Fig. S4†). In addition, photoreactions with different catalyst dosage show that the production of CO is a first order dependence on the concentration of PEI₆-Co (Fig. S5†).

To investigate the synergistic catalysis effect of PEI₆-Co, the reported dinuclear cobalt cryptate Co₂L and mononuclear cobalt CoL¹ complex were chosen as the counterpoints and the photoreactions were carried out under similar conditions (the amount of Co ion was kept same in these catalysts). As shown in Fig. 3a, for PEI₆-Co, the CO product increased nonlinearly under the visible light irradiation, giving an activity of 1170 mmol g^{-1} for CO₂-to-CO conversion (Fig. 3a, black line). This value is almost 2.8 times of mononuclear cobalt catalyst CoL¹ (416 mmol g^{-1} , Fig. 3a, blue line) and comparable with dinuclear cobalt catalyst Co₂L (884 mmol g^{-1} , Fig. 3a, red line), indicating that the easy-to-synthesized coordination polymer

can also achieve the efficient reduction of CO₂ as elaborate molecular catalyst. It is worth noting that when the reaction time reaches 6 h, the evolution rate of CO slows down and even stop. We speculate that the instability of photosensitizer may be a cause of the reaction stopping. Thus we investigate the stability of [Ru(phen)₃](PF₆)₂ before and after the photoreaction using mass spectrometry. The results in Fig. S6 and S7† show that one phenanthroline ligand is substituted by two H₂O molecule after 10 h light irradiation and form [Ru(phen)₂(H₂O)₂](PF₆)₂, which has no effect for CO₂ reduction as photosensitizer. In addition, the tracking of UV-visible absorption spectrum of [Ru(phen)₃](PF₆)₂ shows that the absorbance of [Ru(phen)₃](PF₆)₂ decreases with the light irradiation (Fig. S8†). These results suggest that [Ru(phen)₃](PF₆)₂ decomposed with the light irradiation. In addition, we performed a cyclic stability test on the reaction system by re-adding the photosensitizer [Ru(phen)₃](PF₆)₂ to the stopped photoreactor. The results in Fig. 3b show that with the addition of extra [Ru(phen)₃](PF₆)₂, the photoreaction could restart and the evolution rate of CO is almost maintained, which suggests that the decomposition of [Ru(phen)₃](PF₆)₂ is the main fact for the reduced rate of CO evolution while PEI₆-Co is relatively stable as a photocatalyst for CO₂ conversion in water containing system.

To illustrate the role of each component in the photoreaction, a sequence of control experiments were carried out (Table 2). In the absence of PEI₆-Co, a little amount of CO generated (Table 2, entry 1), indicating that PEI₆-Co was significant to drive the reduction of CO₂ and [Ru(phen)₃](PF₆)₂ could catalyze the conversion of CO₂-to-CO weakly. Further control experiments suggested that the existence of [Ru(phen)₃](PF₆)₂, TEOA, and light was indispensable for the generation of CO (Table 2, entries 2–4). Additionally, when Ar was used as the substitution of CO₂ (Table 2, entries 5), no CO was detected in the photocatalytic system, indicating that the producing of CO was originated from the reduction of CO₂ instead of other organic components.

Conclusions

In summary, based on the synergistic catalytic strategy of dinuclear cobalt, we designed and synthesized a transition metal coordination polymer PEI₆-Co and investigated its catalytic activity towards CO₂ reduction. The results show that because of the effective adsorption of CO₂ by PEI and the synergistic catalytic effect of the adjacent cobalt active sites in PEI₆-Co, the conversion of CO₂-to-CO with high yield of 1170 mmol g^{-1} and selectivity of 95% were achieved in water containing medium. Such performance is almost 2.8 times of mononuclear cobalt catalyst CoL¹ and comparable with dinuclear cobalt catalyst Co₂L. This work provides a prospective strategy for the transformation of molecular catalyst to heterogeneous catalyst in a convenient and cost-effective way.

Conflicts of interest

There are no conflicts to declare.



Acknowledgements

This work was financially supported by NSFC (21702146) and Natural Science Foundation of Tianjin (19JCQNJC05500).

Notes and references

- 1 S. Chen, Y. Qi, C. Li, K. Domen and F. Zhang, *Joule*, 2018, **2**, 2260–2288.
- 2 J. Jian, G. Jiang, R. van de Krol, B. Wei and H. Wang, *Nano Energy*, 2018, **51**, 457–480.
- 3 D. Kim, K. K. Sakimoto, D. Hong and P. Yang, *Angew. Chem., Int. Ed.*, 2015, **54**, 3259–3266.
- 4 A. K. Singh, J. H. Montoya, J. M. Gregoire and K. A. Persson, *Nat. Commun.*, 2019, **10**, 443.
- 5 H. Tong, S. Ouyang, Y. Bi, N. Umezawa, M. Oshikiri and J. Ye, *Adv. Mater.*, 2012, **24**, 229–251.
- 6 C. Gao, Q. Meng, K. Zhao, H. Yin, D. Wang, J. Guo, S. Zhao, L. Chang, M. He, Q. Li, H. Zhao, X. Huang, Y. Gao and Z. Tang, *Adv. Mater.*, 2016, **28**, 6485–6490.
- 7 T. Arai, S. Sato and T. Morikawa, *Energy Environ. Sci.*, 2015, **8**, 1998–2002.
- 8 S. N. Habisreutinger, L. Schmidt-Mende and J. K. Stolarczyk, *Angew. Chem., Int. Ed.*, 2013, **52**, 7372–7408.
- 9 D. C. Grills and E. Fujita, *J. Phys. Chem. Lett.*, 2010, **1**, 2709–2718.
- 10 K. Li, B. Peng and T. Peng, *ACS Catal.*, 2016, **6**, 7485–7527.
- 11 X. Li, J. Yu, M. Jaroniec and X. Chen, *Chem. Rev.*, 2019, **119**, 3962–4179.
- 12 Q.-Q. Bi, J.-W. Wang, J.-X. Lv, J. Wang, W. Zhang and T.-B. Lu, *ACS Catal.*, 2018, **8**, 11815–11821.
- 13 S. Gao, Y. Lin, X. Jiao, Y. Sun, Q. Luo, W. Zhang, D. Li, J. Yang and Y. Xie, *Nature*, 2016, **529**, 68.
- 14 P. S. Nabavi Zadeh, M. Zezzi do Valle Gomes, B. Åkerman and A. E. C. Palmqvist, *ACS Catal.*, 2018, **8**, 7251–7260.
- 15 L.-Y. Wu, Y.-F. Mu, X.-X. Guo, W. Zhang, Z.-M. Zhang, M. Zhang and T.-B. Lu, *Angew. Chem., Int. Ed.*, 2019, **58**, 9491–9495.
- 16 H. Jung, S. Y. Lee, C. W. Lee, M. K. Cho, D. H. Won, C. Kim, H.-S. Oh, B. K. Min and Y. J. Hwang, *J. Am. Chem. Soc.*, 2019, **141**, 4624–4633.
- 17 J. L. White, M. F. Baruch, J. E. Pander, Y. Hu, I. C. Fortmeyer, J. E. Park, T. Zhang, K. Liao, J. Gu, Y. Yan, T. W. Shaw, E. Abelev and A. B. Bocarsly, *Chem. Rev.*, 2015, **115**, 12888–12935.
- 18 R. Kuriki, H. Matsunaga, T. Nakashima, K. Wada, A. Yamakata, O. Ishitani and K. Maeda, *J. Am. Chem. Soc.*, 2016, **138**, 5159–5170.
- 19 R. Kuriki, M. Yamamoto, K. Higuchi, Y. Yamamoto, M. Akatsuka, D. Lu, S. Yagi, T. Yoshida, O. Ishitani and K. Maeda, *Angew. Chem., Int. Ed.*, 2017, **56**, 4867–4871.
- 20 T. Morimoto, T. Nakajima, S. Sawa, R. Nakanishi, D. Imori and O. Ishitani, *J. Am. Chem. Soc.*, 2013, **135**, 16825–16828.
- 21 T. Morimoto, C. Nishiura, M. Tanaka, J. Rohacova, Y. Nakagawa, Y. Funada, K. Koike, Y. Yamamoto, S. Shishido, T. Kojima, T. Saeki, T. Ozeki and O. Ishitani, *J. Am. Chem. Soc.*, 2013, **135**, 13266–13269.
- 22 S. Sato, T. Morika, T. Kajino and O. Ishitani, *Angew. Chem., Int. Ed.*, 2013, **52**, 988–992.
- 23 C. Cometto, R. Kuriki, L. Chen, K. Maeda, T.-C. Lau, O. Ishitani and M. Robert, *J. Am. Chem. Soc.*, 2018, **140**, 7437–7440.
- 24 P. G. Alsabeh, A. Rosas-Hernandez, E. Barsch, H. Junge, R. Ludwig and M. Beller, *Catal. Sci. Technol.*, 2016, **6**, 3623–3630.
- 25 T. Ouyang, H.-H. Huang, J.-W. Wang, D.-C. Zhong and T.-B. Lu, *Angew. Chem., Int. Ed.*, 2017, **56**, 738–743.
- 26 T. Ouyang, H.-J. Wang, H.-H. Huang, J.-W. Wang, S. Guo, W.-J. Liu, D.-C. Zhong and T.-B. Lu, *Angew. Chem., Int. Ed.*, 2018, **57**, 16480–16485.
- 27 V. S. Thoi, N. Kornienko, C. G. Margarit, P. Yang and C. J. Chang, *J. Am. Chem. Soc.*, 2013, **135**, 14413–14424.
- 28 C. Zhao, X. Dai, T. Yao, W. Chen, X. Wang, J. Wang, J. Yang, S. Wei, Y. Wu and Y. Li, *J. Am. Chem. Soc.*, 2017, **139**, 8078–8081.
- 29 E. Torralba-Peñalver, Y. Luo, J.-D. Compain, S. Chardon-Noblat and B. Fabre, *ACS Catal.*, 2015, **5**, 6138–6147.
- 30 H. Takeda, K. Koike, H. Inoue and O. Ishitani, *J. Am. Chem. Soc.*, 2008, **130**, 2023–2031.
- 31 W. Kubo and T. Tatsuma, *J. Am. Chem. Soc.*, 2006, **128**, 16034–16035.
- 32 L. Zong, C. Wang, A. M. P. Moeljadi, X. Ye, R. Ganguly, Y. Li, H. Hirao and C.-H. Tan, *Nat. Commun.*, 2016, **7**, 13455.
- 33 N. P. Mankad, *Chem. – Eur. J.*, 2016, **22**, 5822–5829.
- 34 A. Magnuson, M. Anderlund, O. Johansson, P. Lindblad, R. Lomoth, T. Polivka, S. Ott, K. Stensjo, S. Styring, V. Sundstrom and L. Hammarstrom, *Acc. Chem. Res.*, 2009, **42**, 1899–1909.
- 35 S. Zhang, P. Kang, S. Ubnoske, M. K. Brennaman, N. Song, R. L. House, J. T. Glass and T. J. Meyer, *J. Am. Chem. Soc.*, 2014, **136**, 7845–7848.

